

## Diatom-based water-table reconstruction in boreal peatlands of northeastern China

Xu Chen<sup>1\*</sup>, Suzanne McGowan<sup>2</sup>, Zhao-Jun Bu<sup>3\*</sup>, Xiang-Dong Yang<sup>4</sup>, Yan-Min Cao<sup>5</sup>,  
Xue Bai<sup>1</sup>, Ling-Han Zeng<sup>2</sup>, Jia Liang<sup>1</sup>, Qiang-Long Qiao<sup>1</sup>

1. Hubei Key Laboratory of Critical Zone Evolution, School of Geography and Information Engineering, China University of Geosciences, Wuhan 430074, China

2. School of Geography, University of Nottingham, Nottingham NG7 2RD, UK

3. Institute for Peat and Mire Research, State Environmental Protection Key Laboratory of Wetland Ecology and Vegetation Restoration, Northeast Normal University, Changchun 130024, China

4. State Key Laboratory of Lake Science and Environment, Nanjing Institute of Geography and Limnology, Chinese Academy of Sciences, Nanjing 210008, China

5. College of Resources and Environmental Science, South-Central University for Nationalities, Wuhan 430074, China

\*Corresponding author; e-mail address: xuchen@cug.edu.cn (X. Chen)

buzhaojun@nenu.edu.cn (Z. Bu)

**Abstract:** Peatlands are important ecosystems for biodiversity conservation, global carbon cycling and water storage. Hydrological changes due to climate variability have accelerated the degradation of global and regional ecosystem services of peatlands. Diatoms are important producers and bioindicators in wetlands, but comprehensive diatom-based inference models for palaeoenvironmental reconstruction in peatlands are scarce. To explore the use of diatoms for investigating peatland hydrological change, this study established a training set consisting of diatom composition and twelve environmental factors from 105 surface samples collected from five *Sphagnum* peatlands in northeastern China. Diatom communities were dominated by *Eunotia* species. Ordination analyses showed that depth to the water table (DWT) was the most important factor influencing diatom distribution, independently accounting for 4.99% of total variance in diatom data. Accordingly, a diatom-based DWT transfer function was developed and thoroughly tested. The results revealed that the best-performing model was based on weighted averaging with inverse deshrinking ( $R^2 = 0.66$ , RMSEP = 8.8 cm with leave-one-out cross validation). Quantitative reconstruction of DWT on a short peat core collected from the Aershan Peatland (Inner Mongolia) recorded climate-mediated hydrological changes over the last two centuries. This study presents the first diatom-water table transfer function in *Sphagnum* peatlands, and highlights the potential of diatoms as a powerful tool to assess the magnitude of past hydrological changes in peatlands of northeastern China, as well as similar peat environments worldwide.

**Keywords:** Diatom; training set; transfer function; water-table reconstruction; peatlands; northeastern China

## 1. Introduction

Peatlands are limno-terrestrial ecosystems with habitats intermediate between dry land and water, where the rate of organic matter accumulation is faster than decomposition (Rydin and Jeglum, 2013). They are characterized by a waterlogged soil layer consisting of at least 30% of organic matter and a minimum peat thickness of 30 cm (Charman, 2002). Peatlands cover about 3% of the global land area, but they are unevenly distributed across different climate zones (Minasny et al., 2019). The vast majority of peatlands are in northern latitudes ( $\sim 45^{\circ}$ - $70^{\circ}$  N), where they cover  $\sim 3,200,000$  km<sup>2</sup> of land and store 113-612 gigatonnes of carbon (Loisel et al., 2017; Minasny et al., 2019). This carbon pool is equivalent to about 15-72% of the atmospheric carbon pool (Charman, 2002; Minasny et al., 2019). Dynamics of this large carbon pool exhibit a number of key feedbacks with the global climate system (Charman, 2002). For example, water table drawdown due to climate warming can accelerate aerobic decomposition of peat with greenhouse gas emissions, creating a positive feedback that could further increase warming (Waddington et al., 2015). Studies of peatland hydrology have revealed that hydrological changes may amplify or dampen external interactions between peatlands and the atmosphere (Huang et al., 2018). Hence, understanding of hydrological changes is essential for improving our knowledge of carbon cycling and other related biogeochemical processes in peatlands (Charman, 2002; Rydin and Jeglum, 2013).

Palaeoecological reconstructions provide tools to understand long-term linkages between hydrology-carbon dynamics under changing climate (Zhang et al., 2017; Huang et al., 2018). Depth to the water table is commonly used to summarise peatland hydrology and this metric has been inferred using a range of biotic indicators, such as testate amoebae (protozoans) and plant macrofossils (Charman, 2002; Chambers et al.,

2012). Due to variations in body size, ecology and life history, different organisms respond to hydrological changes at a variety of spatial and temporal scales, e.g. amoebae at the scale of  $\mu\text{m}^3\text{-mm}^3$  and bryophytes at the scale of  $\text{mm}^3\text{-cm}^3$  (Mitchell et al., 2013). Different sensitivities of organisms may cause contradictory reconstructions among proxies (Chambers et al., 2012). For accurate assessment of past hydrological changes, the scientific community has focused considerable attention on retrieving new evidence from peat records.

Diatoms are unicellular, eukaryotic algae that have long been used as a powerful means of deciphering changes in aquatic environments (Battarbee et al., 2000). During recent decades, diatom-based transfer functions have been widely developed to reconstruct a variety of climatic, chemical and hydrological variables in lakes (Smol and Cumming, 2000), while the use of diatoms as a proxy for environmental change in peatlands has lagged far behind lakes (Gaiser and Rühland, 2010). This may partly be due to the dissolution of diatom in many peat sediments or profiles (Bennett and Siegel, 1987). However, long freezing duration may restrict silica recycling, and hence contribute to good preservation of diatom valves in some northern peatlands (Kokfelt et al., 2009).

Although diatoms are an underexploited means for tracking peatland environmental change, the information obtained from fossil diatom assemblages in peatlands has attracted much attention during recent years. For example, diatoms in a Siberian peatland shifted from benthic and alkaliphilic taxa, to epiphytic and acidophilic taxa, and then to aerophilic species, indicating the succession from an open water, to a fen, and then to a bog (Rühland et al., 2000). Fukumoto et al. (2014) found peatland hydroseral succession from fluvial environments in the early Holocene, to a shallow marsh in the mid-Holocene to present fen environments in northern Mongolia. Similar

hydroseral successions were also inferred from diatom records in other northern peatlands (Hargan et al., 2015a; Ma et al., 2018). Collectively, these studies highlight the potential of diatoms as a powerful tool to infer peatland environmental change.

A growing number of contemporary surveys have revealed that diatom assemblages are closely linked to moisture (often expressed as depth to the water table) in surface samples of peatlands (Van de Vijver and Beyens, 1997; Chen et al., 2012; Küttim et al., 2017; Ma et al., 2018). Generally, drought-tolerant taxa (e.g. *Hantzschia amphioxys* (Ehrenberg) Grunow) thrive on dry hummocks, while aquatic species (e.g. *Frustulia saxonica* Rabenhorst) proliferate in moist hollows (Pouličková et al., 2004; Buczkó and Wojtal, 2005; Cantonati et al., 2009, 2011; Chen et al., 2014; Hargan et al., 2015b; Küttim et al., 2017). Modern ecological observations are essential for generating robust and ecologically sound inference models for quantitative reconstruction of the water table (Gaiser and Rühland, 2010). At present, comprehensive diatom-based inference models in peatlands are scarce and clearly needed to reconstruct peatland environmental change. In this study, we aim to (1) establish a regional diatom-water table transfer function using diatom composition and environmental factors measured in surface samples collected from five *Sphagnum* peatlands in northeastern China; (2) apply this transfer function to reconstruct past hydrological change in one site, the Aershan Peatland (Inner Mongolia); (3) evaluate performance and application of the transfer function.

## **2. Materials and methods**

### **2.1 Study area**

The five study sites, i.e. Aershan, Mohe, Tangwanghe, Jinchuan and Hani, all are *Sphagnum*-dominated peatlands in northeastern China (Fig. 1). The landscape of

northeastern China is dominated by the Northeast China Plain in the centre, which is surrounded by mountains, including the Greater Khingan Mountains in the west, the Lesser Khingan Mountains in the north and the Changbai Mountains in the south (Fig. 1). The region is characterized by a temperate continental monsoon climate with long, dry, cold winters and short, moist, cool summers. Mean annual air temperature ranges from -4.4 to 3.3 °C, and average annual precipitation fluctuates between 425 and 740 mm (Zhao, 1999). Mohe and Tangwanghe peatlands lie on the side of the valley bottom, and both of them developed from *Larix gmelinii* (Rupr.) Kuzen forest through paludification (Li et al., 2015). Aershan, Jinchuan and Hani peatlands developed from lava barrier lakes through terrestrialization (Zhang et al., 2019; Ma et al., 2020). Elevations of the sampling sites range from 460 to 1,290 m (Table 1). Water pH in these peatlands is higher than most bogs, while Ca concentrations are within the ranges of bogs and poor fens (Table 1; Rydin and Jeglum, 2013). The vegetation in the five peatlands is dominated by dwarf shrubs, such as *Betula fruticosa* var. *ruprechtiana* Trautv., *Rhododendron tomentosum* Harmaja, *Potentilla fruticosa* L., *Vaccinium uliginosum* L., and different *Sphagnum* mosses such as *S. imbricatum* Hornsch. ex Russ., *S. magellanicum* Brid., *S. fuscum* (Schimp.) Klinggr. and *S. flexuosum* Dozy & Molk. (Lang et al., 1999; Ma et al., 2020).

## 2.2 Field and laboratory methods

A total of 105 surface samples were collected from the five peatlands in August 2016 (Table 1). At each peatland, samples were collected along hydrological transects from hummocks to hollows with two to six samples per transect. At each sampling point, surface *Sphagnum* tufts (the upper 2-3 cm) were cut by scissors and then brought to the laboratory in polyethylene bags. Meanwhile, depth to the water table (DWT) was

measured in a ~ 5 cm diameter hole using a graduated ruler, and water samples were collected from each hole for further analysis. Geographic coordinates of sampling points were determined using a Garmin Etrex GPS. Electrical conductivity (referenced at 25 °C), pH and oxidation-reduction potential (ORP) were measured immediately in water samples collected from the hole using a calibrated portable instrument (HACH HQ40D<sup>®</sup>). Water samples were filtered through a 0.45 µm membrane filter and then refrigerated in the dark until laboratory analysis. Concentrations of NO<sub>3</sub><sup>-</sup> and PO<sub>4</sub><sup>3-</sup> were measured using a continuous-flow autoanalyser (Skalar San Plus<sup>®</sup>), and concentrations of elements (Ca<sup>2+</sup>, K<sup>+</sup>, Mg<sup>2+</sup>, Na<sup>+</sup> and Si) were determined by an inductively coupled plasma-atomic emission spectrometer (PRODIGY SPEC<sup>®</sup>). Total organic carbon (TOC) was measured using a total organic carbon analyser (TORCH<sup>®</sup>). Ten percent of water samples were duplicated as a quality assurance requirement. The reproducibility of the duplicated water samples was >90% for all parameters.

A total of 21 peat samples (each 2 cm thick) were collected from a 42-cm-deep excavated pit in the Aershan Peatland (1290 m a.s.l.), located in the middle section of the Greater Khingan Mountains (Fig. 1). Mean annual ground surface temperature ranges from -1 to 0 °C, and the length of freezing duration is ca. 250 days (Zhao et al., 1999). Diatoms were analysed at 2-cm intervals in this peat sequence. To date the sequence, radioactivities of <sup>210</sup>Pb<sub>total</sub>, <sup>226</sup>Ra and <sup>137</sup>Cs were measured at 4-cm intervals on a gamma spectrometer (Ortec HPGe GWL). *Sphagnum* samples were washed in 100 mL of distilled water and thoroughly squeezed to collect the water with diatoms and mud. This method was advocated by Poulíčková et al. (2004), who compared the washing procedure with mineralization of the whole *Sphagnum* sample, and found the washing method to be ~80% effective. Diatom samples were treated with 30% H<sub>2</sub>O<sub>2</sub> in order to remove organic components. Cleaned valves were mounted in the high

refractive index mountant Naphrax<sup>®</sup>, and at least 300 valves were identified and counted per slide at 1000× magnification using an Olympus<sup>®</sup> BX53 microscope. The diatoms were well preserved in the short peat core, except for some large *Eunotia* species which had broken valves; in this case partial valve tips were summed to calculate a species valve total (Hargan et al., 2015a). Taxonomic identifications were mainly based on Krammer (2000), Kulikovskiy et al. (2010), Liu et al. (2007, 2011), Cantonati et al. (2011), Levkov et al. (2013) and Lange-Bertalot et al. (2011, 2017). *Eunotia paludosa* Grunow was the dominant species in this study, with highly variable valve length (6-53µm) (Lange-Bertalot et al., 2011). Our preliminary work has revealed that valve length of *E. paludosa* is significantly correlated with DWT (Chen et al., 2012), and so this taxon was sub-divided into three morphotypes based on its valve length, including small (6-15 µm), medium (15-30 µm) and large (30-53 µm) types. Chrysophycean stomatocysts were counted concurrently with diatoms in order to calculate a cyst: diatom valve (C: D) ratio (Buczko and Wojtal, 2005).

### 2.3 Data processing and statistical analysis

Taxa with  $\geq 1\%$  abundance in at least one sample were included in the numerical analyses. The calibration dataset consisted of 12 measured environmental variables and 78 diatom taxa from 105 sampling points. All environmental parameters (except pH and DWT) were log-transformed. To explore the species-environment relationship, we applied ordination analyses using the *vegan* package (Oksanen et al., 2019) in R version 3.5.1 (R Core Team, 2018). Detrended correspondence analysis (DCA) was performed on 105 samples to determine whether a unimodal or linear model should be used. A gradient length of 4.98 standard deviations indicated that canonical correspondence analysis (CCA) was suitable to evaluate the relationship between species composition



and explanatory variables (Ter Braak, 1988). A preliminary CCA with all variables was used to reduce the environmental variables to those correlating significantly with diatom composition. Forward selection, with the Monte Carlo tests ( $p < 0.05$ ,  $n = 999$  unrestricted permutations) were used. The relative contribution of each environmental variable was calculated using a series of partial CCAs. The ratio between the first and second eigenvalues ( $\lambda_1/\lambda_2$ ) in CCA ordinations with only one explanatory variable was calculated to assess the explanatory power of the environmental variables (Juggins, 2013).

Weighted averaging (WA), tolerance-downweighted weighted averaging (WA-Tol), weighted average partial least squares (WAPLS) and maximum likelihood (ML) were applied using the *rioja* package (Juggins and Birks, 2012; Juggins, 2017) in R version 3.5.1 (R Core Team, 2018). With respect to WA and WA-Tol models, WA inverse deshrinking (WA.inv) and tolerance downweighted WA.inv (WA.inv.tol) sub-models were chosen for further analysis based on  $R^2$  and the root mean square error of prediction (RMSEP) and average bias. In our dataset, WAPLS had the same outcome as WA, and hence the WAPLS model was not performed further. Transfer functions were first developed for the full dataset, and samples with residuals  $> 20\%$  of overall DWT range were then removed to improve performance (Juggins and Birks, 2012). The general performance of the models was assessed using  $R^2$  and RMSEP with leave-one-out (LOO) cross validation; meanwhile, average and maximum bias was considered. Moreover, leave-one-site-out (LOSO) RMSEP was calculated using the leave-group-out cross-validation function, with sites numbered separately to evaluate the impact of clustered sampling design (Payne et al., 2012). The segment-wise RMSEP<sub>(sw)</sub> approach was used to test the potential impact of uneven sampling along the water table gradient

(Telford and Birks, 2011a). The effect of spatial autocorrelation on the training set was tested using the approach advocated by Telford and Birks (2009).

The transfer function was then applied to the Aershan peat core. The significance of the transfer function reconstruction was tested using the 'random TF' function in the *palaeoSig* package for R language (Telford, 2015). Principal components analysis (PCA) was used to summarise the major underlying changes in the sedimentary diatom assemblages. The correlation coefficient between diatom-inferred DWT and corresponding fossil sample scores on PCA axis 1 was used to further test the validity of the reconstruction (Reavie et al., 2014). Furthermore, the fossil samples were plotted passively on top of a CCA ordination formed by surface diatom composition and significant explanatory variables. Finally, sedimentary records were compared to regional palaeoclimate data of northeastern China (Wang and Xu, 2007).

### **3. Results**

#### 3.1 Calibration dataset

DWT ranged from -4 to 73 cm, representing a gradient from hollows to hummocks (Table 1). The sampling points were generally acidic and deficient in major cations and nutrients. DWT was negatively correlated with pH ( $p < 0.01$ ), but positively correlated with both  $\text{NO}_3^-$  and  $\text{K}^+$  ( $p < 0.01$ ) (Appendix A). A total of 159 taxa belonging to 46 genera were found among the 54,410 identified valves (Appendix B). Species richness ranged from 2 to 47 per sample, with an average of 13. The most common species were *E. paludosa*, *Chamaepinnularia hassiaca* (Krasske) Cantonati et Lange-Bertalot, *Eunotia nymanniana* Grunow, *Eunotia exigua* (Brébisson) Rabenhorst, *Nitzschia acidoclinata* Lange-Bertalot, *H. amphioxys*, *Luticola pseudoimbricata* sp. nov., *Kobayasiella parasubtilissima* (Kobayasi et Nagumo) Lange-Bertalot, *Tabellaria*

*flocculosa* (Roth) Kützing, *Eunotia mucophila* (Lange-Bertalot et Nörpel) Lange-Bertalot, *Eunotia bilunaris* (Ehrenberg) Schaarschmidt, *Eunotia superpaludosa* Lange-Bertalot, *Fragilariforma constricta* (Ehrenberg) Williams et Round, *Pinnularia borealis* Ehrenberg, *Microcostatus maceria* (Schimanski) Lange-Bertalot, *F. saxonica*, *Chamaepinnularia mediocris* (Krasske) Lange-Bertalot (Fig. 2 and Appendix C). The genera with the most species were *Eunotia* (36 species) and *Pinnularia* (25 species). 78 taxa ( $\geq 1\%$ ) were included in the dataset, representing 90-100% of the total percentage of each sample.

### 3.2 Ordination analysis

The first and second DCA axis explained 15.1% and 11.2% of total variance in diatom composition, respectively. The DCA biplot showed considerable assemblage overlap between different sites (Fig. 3), although Mohe and Tangwanghe peatlands occupied a slightly lower position on axis 2. This is probably due to relatively high abundances of *E. paludosa* large type and *E. superpaludosa* in the two peatlands. Overall the DCA biplot confirms the broad distribution of many taxa as they overlap between different peatlands.

A preliminary CCA indicated that DWT, Na<sup>+</sup>, Si, TOC, pH and PO<sub>4</sub><sup>3-</sup> formed the minimum group of significant variables and explained 16% of total variance in diatom composition (Fig. 4 and Table 2). Samples of each peatland (except TWH) mainly separated horizontally along the CCA axis 1 that represented the water table gradient (Fig. 4A). The results of the ratios of  $\lambda_1$  to  $\lambda_2$  ( $\lambda_1/\lambda_2 = 0.56$ ) revealed that DWT was most strongly correlated with diatom composition, followed by Na<sup>+</sup> (0.33), PO<sub>4</sub><sup>3-</sup> (0.22), pH (0.21), TOC (0.20) and Si (0.19) (Table 2). The ratios for each of the six environmental factors were not greatly altered when the other variables were selected as covariables.

In partial CCAs with five of the six significant environmental factors as covariables and the remaining significant factor as the sole explanatory variable, DWT independently accounted for the largest part of total variance in diatom data (4.99%), followed by Si (2.2%), pH (2.0%), Na<sup>+</sup> (1.7%), TOC (1.7%) and PO<sub>4</sub><sup>3-</sup> (1.4%) (Table 2). Both the  $\lambda_1/\lambda_2$  ratio and the amount of variance explained by the sole effect of each variable suggest that DWT should be the most important variable accounting for diatom distribution, and it could be used to generate a diatom-based DWT transfer function.

### 3.3 DWT inference model

The performance statistics of the transfer function models are given in Table 3. The number of samples with residuals > 20% of overall DWT range (77 cm) varied for each model type. After removing these samples, the performance of most models improved, i.e. an increase in  $R^2$  and a decrease in RMSEP. The WA.inv model outperformed other models for predicting DWT (RMSEP<sub>(LOO)</sub> = 8.8 cm,  $R^2$  = 0.66). The correlation between observed and predicted DWT (Fig. 5) indicated most samples with high residual values were from two segments (10-20 cm and 40-70 cm). WA.inv model-based DWT optima and tolerance patterns of the major species are presented in Fig. 6. *Luticola nivalis* (Ehrenberg) Mann, *Luticola acidoclinata* Lange-Bertalot, *L. pseudoimbricata*, *E. fallax*, *H. amphioxys* and *P. borealis* were indicators of dry hummocks, while *N. acidoclinata*, *Hantzschia calcifuga* Reichardt et Lange-Bertalot, *Nitzschia terrestris* (Petersen) Lund and *E. bilunaris* preferred wet hollows. Generally, drought-tolerant species had larger tolerance ranges than aquatic species.

RMSEP<sub>(LOSO)</sub> values were higher than RMSEP<sub>(LOO)</sub> for each of the three models (Table 3), suggesting that the clustered characteristics of the training set had potential influences on RMSEP values. The RMSEP<sub>(SW)</sub> values produced by the WA.inv model

are presented in Fig. 7. The  $RMSEP_{(sw)}$  values for the segments (10-20 cm and 40-70 cm) were relatively high compared to those for other segments. The effect of spatial autocorrelation on all of the models was tested and showed that  $R^2$  value was lower with neighbourhood deletion than with random deletion for each model (Fig. 8). This means that nearby sites are not equivalent to a random set of sites. Model performance was worse when environmentally similar sites were deleted than when the same number of sites was deleted according to geographical distance (Fig. 8).

### 3.4 Diatom stratigraphy and water-table reconstruction in the Aershan Peatland

In the Aershan peat core, activities of  $^{137}Cs$  generally decreased with depth, without the fallout peak that can be used to identify the 1963 depth (Fig. 9A). The peak activity of  $^{137}Cs$  was observed in surface sediment, probably affected by diffusion through pore water as well as biological uptake by *Sphagnum* (Turetsky et al., 2004).  $^{210}Pb_{total}$  reached a radioactive equilibrium value that was greater than  $^{226}Ra$  (Fig. 9B), probably due to an efficiency calibration error with the gamma spectrometers. Supported  $^{210}Pb$  activity was calculated from the mean asymptotic activity in the bottom layers (Fig. 9B). Unsupported  $^{210}Pb_{ex}$  was calculated by subtracting the mean asymptotic activity from  $^{210}Pb_{total}$ , and the plot of the logarithm of  $^{210}Pb_{ex}$  against depth was closely approximated by a straight line (Fig. 9C). Hence, the chronology can be calculated using the constant flux constant sedimentation model (cf. Appleby, 2001). The 42-cm long sediment core spanned the last ~200 years, with a mean sedimentation rate of 1.93 mm year<sup>-1</sup> (Fig. 9D).

Three distinct zones were identified in the diatom stratigraphy based on cluster analysis (Fig. 10). Zone I (ca.1793-1933 AD) was co-dominated by *Encyonema groenlandica* (Foged) Kulikovskiy et Lange-Bertalot, *E. exigua*, *Eunotia groenlandica*

(Grunow) Nörpel-Schempp et Lange-Bertalot, *Eunotia valida* Hustedt and *H. amphioxys*, with some fluctuations. In Zone II (ca.1933-1975 AD), diatom composition was relatively stable, characterized by high percentages of *Encyonema groenlandica* and *E. fallax* and frequent occurrence of *Encyonopsis amphioxys* (Kützing) Liu et Shi, *Eunotia bidens* Ehrengerg, *E. valida*, *Neidium bisulcatum* (Lagerstedt) Cleve and *Pinnularia crucifera* Cleve-Euler. Zone III (ca.1975-2016 AD) was characterized by increasing abundances of *C. hassiaca*, *E. nymanniana*, *H. amphioxys* and *P. borealis*, with synchronous decreases in *E. fallax* and *Encyonema groenlandica*. Diatom-inferred DWT displayed a broad increase before the 1990s, except several episodes of low values (Fig. 11A). The random TF tests indicated that the WA.inv model was statistically insignificant at  $p > 0.05$ . In order to test the predictive power of our transfer function, we compared the reconstructed DWT with C: D ratio, sample scores on PCA axis 1 and independent climatic data (Fig. 11). Sample scores on PCA axis 1 showed significant correlations with diatom-inferred DWT ( $r = -0.47$ ,  $p < 0.05$ ) and C: D ratio ( $r = -0.60$ ,  $p < 0.01$ ). Furthermore, fossil samples (except the surface sample) were mainly displayed along the first CCA axis of the modern training set in the passive CCA (Fig. 12). Within the radionuclide age uncertainties, synchronous low values in both diatom-inferred DWT and C: D ratio and high sample scores on PCA1 broadly corresponded to an increase in flood frequency during the episodes of 1810-1840 AD, 1900-1910 AD and 1940-1970 AD.

## **4. Discussion**

### **4.1 Diatom distribution in *Sphagnum* peatlands**

The relationships between species and environmental gradients within peatlands are well known for vascular plants (Jiroušek et al., 2013), mosses (Clymo and Hayward,

1982) and testate amoebae (Charman, 2002), but the ecology of peatland diatoms is less well investigated (Gaiser and Rühland, 2010). In the semi-terrestrial and acidic environments of peatlands, organisms are more or less resistant to both low pH and desiccation (Rydin and Jeglum, 2013). Both pH and TOC were significantly correlated with diatom composition. Water pH is the primary factor influencing diatom distribution in Western Carpathian spring fens (Fránková et al., 2009), Alpine mires (Cantonati et al., 2011) and Canadian peatlands (Hargan et al., 2015b). *Sphagnum* mosses, the dominant plants in boreal peatlands, contain a number of uronic and phenolic acids that can exchange hydrogen ions for cations in water at the carboxyl group (Clymo and Hayward, 1982). Due to the organic acids produced by *Sphagnum*, peatlands gradually undergo a natural acidification (Rydin and Jeglum, 2013). In this study, water pH was significantly correlated with TOC ( $r = -0.85$ ,  $p < 0.001$ ). In our study sites, *E. paludosa* and *K. parasubtilissima* preferred more acidic habitats, while *T. flocculosa* and *E. nymanniana* mainly occur in less acidic environments.

Silica, phosphate and sodium were also found to be significant environmental factors for diatom distribution. Silica is a key nutrient for diatom valve-building and hence is a limiting factor for diatom growth in peatlands (Fránková et al., 2009; Cantonati et al., 2011; Hájková et al., 2011). Although its concentrations in our study sites never reach limiting values ( $< 0.1 \text{ mg L}^{-1}$ ) (Cantonati et al. 2006), diatom distribution was significantly correlated with Si. For example, samples with low Si concentrations in Hani Peatland were dominated by lightly silicified diatoms (e.g. *E. paludosa* small type). A significant relationship between  $\text{Na}^+$  concentration and diatom composition was also found by Jiroušek et al. (2013) and Chen et al. (2016). In comparison with halophobe diatom species, oligohalobous taxa (e.g. *E. bilunaris*, *N. terrestris* and *Humidophila contenta* (Grunow) Lowe, Kociolek, Johansen, Van de

Vijver, Lange-Bertalot et Kopalová) preferred habitats with higher Na<sup>+</sup> concentrations in this study (Fig. 4). Sodium is probably related not only to salinity or nutrition, but it may covary with some causally important variables (Jiroušek et al., 2013). In our sampling sites, sodium is positively correlated with calcium, potassium and magnesium ( $r > 0.21$ ,  $p < 0.05$ ). These base cations are generally limiting factors for plant growth in peatlands (Rydin and Jeglum, 2013). Because diatoms are primarily photoautotrophic organisms, they are directly affected by changes in availability of nutrients and light (Smol and Cumming, 2000). Because the peat surface is gradually cut off from the mineral soil, the total amount of phosphorus tends to be low in peatlands (Rydin and Jeglum, 2013). Phosphate has been reported to be a limiting nutrient for diatom growth in European peatlands (Jiroušek et al., 2013).

Surface topography of *Sphagnum* peatlands is frequently hummocky, with elevated mounds alternating with flatter, wetter hollows (Charman, 2002). The moisture gradient from wet hollows to dry hummocks was generally found to be a primary factor influencing diatom composition (Van de Vijver and Beyens, 1997; Pouličková et al., 2004; Cantonati et al., 2009, 2011; Chen et al., 2012). Xerophytic species such as *E. paludosa* small type, *H. amphioxys*, *P. borealis*, and *L. nivalis* were mainly observed on elevated hummocks that periodically dry out. These well-known terrestrial and aerophilic diatoms are commonly found on surface soils, tree barks and even on hot desert surfaces (Johansen, 2010). The large, medium and small types of *E. paludosa* had DWT optima of 24, 27 and 33 cm, respectively. Diatom cell size tends to decrease in dry hummocks of peatlands, which could be a response to drought in the extreme habitats (Chen et al., 2012). A very similar association of diatom cell size and moisture were described in peatlands of Canada (Hargan et al., 2015a) and South Georgia (Van de Vijver and Beyens, 1997). In contrast to the desiccation-tolerant species, *N.*



*acidoclinata*, *E. bilunaris* and *E. incisa* thrive in wet hollows. Generally, diatom assemblages are distinguishable along the water table gradient due to species-specific responses to periodic drying (Cantonati et al., 2011).

#### 4.2 Potential for hydrological reconstruction

Based on the ratio of  $\lambda_1/\lambda_2$  and unique effect of each significant variable, DWT is the most important factor influencing diatom distribution. The ratio  $\lambda_1/\lambda_2$  of DWT was lower than the criterion ( $\lambda_1/\lambda_2 = 1$ ) advised by Ter Braak (1988), indicating that caution should be taken with building a transfer function (Juggins, 2013). Several studies suggest that variables which do not fit this criterion may still be useful, but more critical assessment of the reconstructions is needed (Curtis et al., 2009; Gomes et al., 2014).

The WA.inv model had smaller  $\text{RMSEP}_{(\text{LOO})}$  and larger  $R^2$  than other models (Table 3), and these values in all our models were reasonable in comparison with the testate amoeba-based DWT transfer functions in boreal peatlands (Li et al., 2015; Payne et al., 2016). The performance was worse when neighbouring sites were deleted than with random deletion (Fig. 8), indicating that spatial autocorrelation existed due to the clustered characteristics of the dataset. Our training set only had five sites, and the number of sampling points in each site ranged from 9 to 37. This means that LOSO cross validation removed approximately one-twelfth to one-third of samples from the training set. This over-removal likely contributes to the deterioration of model performance with LOSO cross validation (Li et al., 2015). When considering the results of  $\text{RMSEP}_{(\text{LOSO})}$  and spatial autocorrelation (Fig. 8 and Table 3), the WA.inv model performed best and hence it was selected for water table reconstruction. However, the transfer function overestimated DWT at wet sites, and underestimated it at dry sites (Fig. 5). At the sites with high residuals, diatom assemblages were characterized by

high abundance of *E. paludosa* large type, which had a DWT optimum of 24 cm in our training set. The dominance of *E. paludosa* large type (> 50%) at relatively dry (DWT: 40-70 cm) or wet (DWT: 10-20 cm) sites probably led to high residuals. In addition, *E. paludosa* large type preferred habitats with high concentrations of  $\text{PO}_4^{3-}$ , TOC and Si, indicating that the distribution of this species may be influenced by nutrients.

*Sphagnum* turfs in the top 2-3 cm contain a time-averaged diatom assemblage that spans several months (Clymo and Hayward, 1982). Similar to testate amoebae-based calibration sets (Mitchell et al., 2013; Qin et al., 2013; Payne et al., 2016), our training set was established using single measurements of environmental factors. Water-table monitoring data of *Sphagnum* peatlands in the Lesser Khingan Mountains (next to the Tangwanghe Peatland) revealed that water table was relatively stable during the growing season, except for visible changes during the thawing and freezing processes (Sun et al., 2011). In a *Sphagnum* peatland in Northern Poland, seasonal patterns of testate amoebae communities were significantly correlated with seasonal dynamics in the water table (Marcisz et al., 2014). Hence, the residuals probably reflect fluctuations around the mean water table depth. In addition, it is likely that DWT is decoupled from moisture conditions on dry hummocks (Zhang et al., 2017), because water collection from humid air by *Sphagnum* would increase the moisture content in the microhabitat for diatom growth. For example, *S. fuscum* can maintain high moisture content for microorganisms living on its leaves in relatively dry hummocks (Mitchell et al., 2013). Due to the effects of steep resource gradients of nutrient and light availability in limno-terrestrial peatland habitats (Fránková et al., 2009; Hájková et al., 2011; Jiroušek et al., 2013), diatoms may be influenced by other environmental factors besides DWT. For example, Fránková et al. (2019) found that conductivity and pH were the most

important variables responsible for diatom distribution along the mineral richness gradient in Carpathian peatlands.

The WA.inv model gave a non-significant reconstruction ( $p > 0.05$ ), indicating that the reconstruction should be interpreted with caution based on the cut-off value proposed by Telford and Birks (2011b). One potential explanation is that fossil samples had poor analogues with the modern calibration samples, as percentages of *Encyonema groenlandica*, *E. fallax* and *E. praerupta* were greater than those in the modern data set. Similarly, the results of random TF tests on a large number of testate amoebae-based DWT reconstructions revealed that a substantial majority (25 of 30) of these studies gave non-significant results (Payne et al., 2016). Although a non-significant random TF  $p$ -value limits the validity of the reconstructions, significant correlations between fossil sample scores on PCA axis 1 and diatom-inferred DWT, and C: D ratio could provide a more detailed and critical assessment of the reconstructions (Reavie et al., 2014). In addition, the distribution of fossil samples along the first axis of the passive CCA could further validate the reconstructions (Fig. 12).

#### 4.3 Past water-table change in the Aershan Peatland

Similar trends were observed in DWT, C: D ratio and sample scores on PCA axis 1 from the peat core (Fig. 11). Generally, C: D ratio is high in periodically desiccated conditions, as chrysophytes can produce a large number of cysts in order to withstand these harsh environments (Buczko and Wojtal, 2005). Compared with chrysophytes, diatoms are generally less competitive in drier and mossy habitats (Rühland et al., 2000). During the three wet episodes of 1810-1840 AD, 1900-1910 AD and 1940-1970 AD, low values in DWT and C: D ratio and high sample scores on PCA axis 1 coincided with an increase in flooding frequency (Fig. 11). *Encyonema groenlandica*, *N.*

*bisulcatum* and *P. crucifera* were abundant during these wet periods, and these species had relatively low DWT optima in comparison with other dominant species in the peat core (Fig. 6). The increase in DWT and C: D ratio and the decrease in PCA scores between the 1970s and the 1990s broadly coincided with an increase in drought frequency (Fig. 11). Taken together, diatom-inferred DWT agreed with climate-mediated hydrological change in peatlands.

## 5. Conclusions

Future climate warming will accelerate permafrost thawing and evaporation in peatlands, and contribute to fluctuations in the water table. Understanding the processes and mechanisms of these oscillations is crucial for facilitating sustainable peatland management and understanding the relations between climate change and peatland hydrology.

- Surface diatom assemblages and physicochemical factors in five *Sphagnum* peatlands (NE China) were used to build a diatom water-table transfer function which was applied to a peat core collected from the Aershan Peatland (Inner Mongolia).
- Diatom-inferred water-table changes over the last two century agreed with sedimentary sample scores on PCA axis 1 and regional palaeoclimate data by identifying wetter conditions during 1810-1840 AD, 1900-1910 AD and 1940-1970 AD.
- The diatom-water table transfer function provides a novel tool that will facilitate future studies on palaeohydrology reconstruction in peatlands of northeastern China, as well as similar peat environments worldwide.

- The present study mainly focuses on five peatlands, but expanding the diatom training set to encompass more peatland sites should improve the performance of the transfer function models.
- Due to the effects of monsoonal climate, seasonal changes in environmental conditions will contribute to temporal changes in diatom assemblages in peatlands. Little knowledge exists on the seasonality of diatoms in these peatlands, and future endeavours in this field would be helpful to learn about the ecology of peatland diatoms.
- Given the alarming rate of global peatland loss and resultant ecological and societal repercussions, the use of diatoms as proxies of peatland environmental changes should be better exploited, especially in the rapidly developing countries.

### **Acknowledgements**

We acknowledge Zhao Li, Yue Yan-An, Ma Jin-Ze, Chai Xin-Na, Liu Yi-Lan, Zhu Yu-Xin, Xia Wei-Lan for field and laboratory assistance. This study was supported by the National Natural Science Foundation of China (41572343 and 41877428), the Open Fund of the State Environmental Protection Key Laboratory of Wetland Ecology and Vegetation Restoration, Northeast Normal University and Jilin Provincial Science and Technology Development Project (20190101025JH). We are grateful to constructive comments and suggestions from anonymous reviewers and handling editor.

**Appendix A** Multipanel display of pairwise relationships between environmental variables.

**Appendix B** List of all taxa observed in the training set.

## **Appendix C** LM micrographs of main diatom species in the study area.

### **References**

- Appleby, P.G. (2001) Tracking Environmental Change Using Lake Sediments. Last, W. and Smol, J. (eds), pp. 171-203, Springer Netherlands.
- Battarbee, R.W. (2000) Palaeolimnological approaches to climate change, with special regard to the biological record. *Quaternary Science Reviews* 19(1-5), 107-124.
- Bennett, P., Siegel, D.I. (1987) Increased solubility of quartz in water due to complexing by organic compounds. *Nature* 326, 684.
- Buczko, K., Wojtal, A. (2005) Moss inhabiting siliceous algae from Hungarian peat bogs. *Studia Botanica Hungarica* 36, 21-42.
- Cantonati, M., Gerecke, R., Bertuzzi, E. (2006) Springs of the Alps – Sensitive Ecosystems to Environmental Change: From Biodiversity Assessments to Long-term Studies. *Hydrobiologia* 562(1), 59-96.
- Cantonati, M., Lange-Bertalot, H., Decet, F., Gabrieli, J. (2011) Diatoms in very-shallow pools of the site of community importance Danta di Cadore Mires (south-eastern Alps), and the potential contribution of these habitats to diatom biodiversity conservation. *Nova Hedwigia* 93(3-4), 475-507.
- Cantonati, M., Van de Vijver, B., Lange - Bertalot, H. (2009) *Microfissurata* gen. nov.(bacillariophyta), a new diatom genus from dystrophic and intermittently wet terrestrial habitats. *Journal of Phycology* 45(3), 732-741.
- Chambers, F.M., Booth, R.K., De Vleeschouwer, F., Lamentowicz, M., Le Roux, G., Mauquoy, D., Nichols, J.E., van Geel, B. (2012) Development and refinement of proxy-climate indicators from peats. *Quaternary International* 268(0), 21-33.
- Charman, D. (2002) Peatlands and environmental change, John Wiley & Sons, Ltd.

- Chen, X., Bu, Z., Stevenson, M.A., Cao, Y., Zeng, L., Qin, B. (2016) Variations in diatom communities at genus and species levels in peatlands (central China) linked to microhabitats and environmental factors. *Science of the Total Environment* 568, 137-146.
- Chen, X., Bu, Z., Yang, X., Wang, S. (2012) Epiphytic diatoms and their relation to moisture and moss composition in two montane mires, Northeast China. *Fundamental and Applied Limnology* 181(3), 197-206.
- Chen, X., Qin, Y., Stevenson, M.A., McGowan, S. (2014) Diatom communities along pH and hydrological gradients in three montane mires, central China. *Ecological Indicators* 45(0), 123-129.
- Curtis, C.J., Juggins, S., Clarke, G., Battarbee, R.W., Kernan, M., Catalan, J., Thompson, R., Posch, M. (2009) Regional influence of acid deposition and climate change in European mountain lakes assessed using diatom transfer functions. *Freshwater Biology* 54(12), 2555-2572.
- Clymo, R.S., Hayward, P.M. (1982) *Bryophyte Ecology*. Smith, A.J.E. (ed), pp. 229-289, Springer Netherlands.
- Fránková, M., Bojková, J., Pouličková, A., Hájek, M. (2009) The structure and species richness of the diatom assemblages of the Western Carpathian spring fens along the gradient of mineral richness. *Fottea* 9(2), 355-368.
- Fukumoto, Y., Kashima, K., Ganzorig, U. (2014) The Holocene environmental changes in boreal fen peatland of northern Mongolia reconstructed from diatom assemblages. *Quaternary International* 348, 66-81.
- Gaiser, E., Rühland, K. (2010) Diatoms as indicators of environmental change in wetlands and peatlands. In: Smol, J.P., Stoermer, E.F. (eds), *The diatoms:*

- applications for the environmental and earth sciences, pp. 473-496, Cambridge University Press.
- Gomes, D.F., Albuquerque, A.L.S., Torgan, L.C., Turcq, B., Sifeddine, A. (2014) Assessment of a diatom-based transfer function for the reconstruction of lake-level changes in Boqueirão Lake, Brazilian Nordeste. *Palaeogeography, Palaeoclimatology, Palaeoecology* 415, 105-116.
- Hájková, P., Bojková, J., Fránková, M., Opravilová, V., Hájek, M., Kintrová, K., Horskák, M. (2011) Disentangling the effects of water chemistry and substratum structure on moss-dwelling unicellular and multicellular micro-organisms in spring-fens. *Journal of Limnology* 70, 54-64.
- Hargan, K.E., Rühland, K.M., Paterson, A.M., Holmquist, J., MacDonald, G.M., Bunbury, J., Finkelstein, S.A., Smol, J.P. (2015a) Long-term successional changes in peatlands of the Hudson Bay Lowlands, Canada inferred from the ecological dynamics of multiple proxies. *The Holocene* 25(1), 92-107.
- Hargan, K.E., Rühland, K.M., Paterson, A.M., Finkelstein, S.A., Holmquist, J.R., MacDonald, G., Keller, W., Smol, J.P. (2015b) The influence of water table depth and pH on the spatial distribution of diatom species in peatlands of the Boreal Shield and Hudson Plains, Canada. *Botany* 93(2), 57-74.
- Huang, X., Pancost, R.D., Xue, J., Gu, Y., Evershed, R.P., Xie, S. (2018) Response of carbon cycle to drier conditions in the mid-Holocene in central China. *Nature Communications* 9(1), 1369.
- Jiroušek, M., Pouličková, A., Kintrová, K., Opravilová, V., Hájková, P., Rybníček, K., Kočí, M., Bergová, K., Hnilica, R., Mikulášková, E., Králová, Š., Hájek, M. (2013) Long-term and contemporary environmental conditions as determinants of the species composition of bog organisms. *Freshwater Biology* 58(10), 2196-2207.



- Johansen, J.R. (2010). Diatoms of aerial habitats. In: Stoermer, E.F., Smol, J.P. (eds), *The Diatoms Applications for the Environmental and Earth Sciences* (2nd Edition), pp. 465-472, Cambridge University Press, Cambridge.
- Juggins, S. (2013) Quantitative reconstructions in palaeolimnology: new paradigm or sick science? *Quaternary Science Reviews* 64(0), 20-32.
- Juggins, S. (2017) rioja: Analysis of Quaternary Science Data, R package version (0.9-15.1).
- Juggins, S., Birks, H.J.B. (2012) *Tracking Environmental Change Using Lake Sediments: Data Handling and Numerical Techniques*. Birks, H.J.B., Lotter, A.F., Juggins, S., Smol, J.P. (eds), pp. 431-494, Springer Netherlands, Dordrecht.
- Kokfelt, U., Struyf, E., Randsalu, L. (2009) Diatoms in peat – Dominant producers in a changing environment? *Soil Biology and Biochemistry* 41(8), 1764-1766.
- Krammer, K. (2000) *Diatoms of Europe Volume 1: The genus Pinnularia*, ARG Gantner Verlag KG, Postfach.
- Kulikovskiy, M.S., Lange-Bertalot, H., Witkowski, A., Dorofeyuk, N.I., Genkal, S.I. (2010) Diatom assemblages from *Sphagnum* bogs of the world. I. Nur bog in northern Mongolia, J. Cramer, Stuttgart, Germany.
- Küttim, L., Küttim, M., Puusepp, L., Sugita, S. (2017) The effects of ecotope, microtopography and environmental variables on diatom assemblages in hemiboreal bogs in Northern Europe. *Hydrobiologia* 792(1), 137-149.
- Lang, H., Zhao, K., Chen, K. (1999) *Wetland vegetation in China*, Science Press, Beijing.
- Lange-Bertalot, H., Bak, M., Witkowski, A., Tagliaventi, N. (2011) *Diatoms of Europe Vol. 6: Eunotia and some related genera*, ARG Gantner Verlag KG, Postfach.

- Lange-Bertalot, H., Hofmann, G., Werum, M. and Cantonati, M. (2017) Freshwater Benthic Diatoms of Central Europe. Over 800 common species used in ecological assessment. Koeltz Botanical Books, Königstein.
- Lange-Bertalot, H., Krammer, K. (2001) Diatoms of Europe volume 2: *Navicula* sensu stricto, 10 genera separated from *Navicula* sensu lato, ARG Gantner Verlag KG, Postfach.
- Levkov, Z., Metzeltin, D. and Pavlov, A. (2013) Diatoms of Europe Volume 7: *Luticola* and *Luticolopsis*, Koeltz Scientific Books, Königstein.
- Li, H., Wang, S., Zhao, H., Wang, M. (2015) A testate amoebae transfer function from *Sphagnum*-dominated peatlands in the Lesser Khingan Mountains, NE China. *Journal of Paleolimnology* 54(2-3), 189-203.
- Liu, Y., Wang, Q.X., Fu, C.X. (2011) Taxonomy and distribution of diatoms in the genus *Eunotia* from the Da'erbin Lake and Surrounding Bogs in the Great Xing'an Mountains, China. *Nova Hedwigia* 92(1-2), 205-232.
- Liu, Y., Wang, Q.X., Shi Z.X. (2007) Newly Recorded Species of Cymbellaceae (Bacillariophyta) from Da'erbin Lake Daxing'anling Mountains, China. *Journal of Wuhan Botanical Research* 25(6): 565-571.
- Loisel, J., van Bellen, S., Pelletier, L., Talbot, J., Hugelius, G., Karran, D., Yu, Z., Nichols, J., Holmquist, J. (2017) Insights and issues with estimating northern peatland carbon stocks and fluxes since the Last Glacial Maximum. *Earth-Science Reviews* 165, 59-80.
- Ma, J.Z., Chen, X., Malik, A., Bu, Z.J., Zhang, M.M., Wang, S.Z., Sundberg, S. (2020) Environmental together with interspecific interactions determine bryophyte distribution in a protected mire of Northeast China. *Frontier in Earth Science* 8, 32.

- Ma, L., Gao, C., Kattel, G.R., Yu, X., Wang, G. (2018) Evidence of Holocene water level changes inferred from diatoms and the evolution of the Honghe Peatland on the Sanjiang Plain of Northeast China. *Quaternary International* 476, 82-94.
- Marcisz, K., Lamentowicz, Ł., Słowińska, S., Słowiński, M., Muszak, W., Lamentowicz, M. (2014) Seasonal changes in Sphagnum peatland testate amoeba communities along a hydrological gradient. *European Journal of Protistology* 50, 445-455.
- Minasny, B., Berglund, Ö., Connolly, J., Hedley, C., de Vries, F., Gimona, A., Kempen, B., Kidd, D., Lilja, H., Malone, B., McBratney, A., Roudier, P., O'Rourke, S., Rudiyanto, Padarian, J., Poggio, L., ten Caten, A., Thompson, D., Tuve, C., Widyatmanti, W. (2019) Digital mapping of peatlands – A critical review. *Earth-Science Reviews* 196, 102870.
- Mitchell, E.A.D., Payne, R.J., van der Knaap, W.O., Lamentowicz, Ł., Gąbka, M., Lamentowicz, M. (2013) The performance of single- and multi-proxy transfer functions (testate amoebae, bryophytes, vascular plants) for reconstructing mire surface wetness and pH. *Quaternary Research* 79(1), 6-13.
- Oksanen, J., Blanchet, F.G., Friendly, M., Kindt, R., Legendre, P., McGlenn, D., Minchin, P.R., O'Hara, R. B., Simpson, G.L., Solymos, P., Stevens, M.H.H., Szoecs, E., Wagner, H. (2019). *vegan: Community Ecology Package*. R package version 2.5-4. <https://CRAN.R-project.org/package=vegan>
- Payne, R.J., Babeshko, K.V., van Bellen, S., Blackford, J.J., Booth, R.K., Charman, D.J., Ellershaw, M.R., Gilbert, D., Hughes, P.D.M., Jassey, V.E.J., Lamentowicz, Ł., Lamentowicz, M., Malysheva, E.A., Mauquoy, D., Mazei, Y., Mitchell, E.A.D., Swindles, G.T., Tsyganov, A.N., Turner, T.E., Telford, R.J. (2016) Significance

- testing testate amoeba water table reconstructions. *Quaternary Science Reviews* 138, 131-135.
- Payne, R.J., Telford, R.J., Blackford, J.J., Blundell, A., Booth, R.K., Charman, D.J., Lamentowicz, Ł., Lamentowicz, M., Mitchell, E.A.D., Potts, G., Swindles, G.T., Warner, B.G., Woodland, W. (2012) Testing peatland testate amoeba transfer functions: Appropriate methods for clustered training-sets. *The Holocene* 22(7), 819-825.
- Pouličková, A., Hájková, P., Krenková, P., Hájek, M. (2004) Distribution of diatoms and bryophytes on linear transects through spring fens. *Nova Hedwigia* 78(3-4), 411-424.
- Qin, Y., Mitchell, E.D., Lamentowicz, M., Payne, R., Lara, E., Gu, Y., Huang, X., Wang, H. (2013) Ecology of testate amoebae in peatlands of central China and development of a transfer function for paleohydrological reconstruction. *Journal of Paleolimnology* 50(3), 319-330.
- Reavie, E.D., Heathcote, A.J., Shaw Chraïbi, V.L. (2014) Laurentian Great Lakes Phytoplankton and Their Water Quality Characteristics, Including a Diatom-Based Model for Paleoreconstruction of Phosphorus. *Plos One* 9(8), e104705.
- Rühland, K., Smol, J.P., Jasinski, J.P., Warner, B.G. (2000) Response of diatoms and other siliceous indicators to the developmental history of a peatland in the Tiksi Forest, Siberia, Russia. *Arctic, Antarctic, and Alpine Research* 32, 167-178.
- Rydin, H., Jeglum, J.K. (2013) *The Biology of Peatlands* (2nd edition), Oxford University Press.
- Smol, J.P., Cumming, B.F. (2000) Tracking long-term changes in climate using algal indicators in lake sediments. *Journal of Phycology* 36(6), 986-1011.

- Sun, X., Mu, C., Song, C. (2011) Seasonal and spatial variations of methane emissions from montane wetlands in Northeast China. *Atmospheric Environment* 45, 1809-1816.
- R Core Team. (2018) R: A language and environment for statistical computing. R Foundation for Statistical Computing, Vienna, Austria.
- Telford, R.J. (2015) palaeoSig: Significance Tests of Quantitative Palaeoenvironmental Reconstructions, R package version (1.1-3).
- Telford, R.J., Birks, H.J.B. (2009) Evaluation of transfer functions in spatially structured environments. *Quaternary Science Reviews* 28(13), 1309-1316.
- Telford, R.J., Birks, H.J.B. (2011a) Effect of uneven sampling along an environmental gradient on transfer-function performance. *Journal of Paleolimnology* 46(1), 99.
- Telford, R.J., Birks, H.J.B. (2011b) A novel method for assessing the statistical significance of quantitative reconstructions inferred from biotic assemblages. *Quaternary Science Reviews* 30(9-10), 1272-1278.
- Ter Braak, C.J. (1988) CANOCO-a FORTRAN program for canonical community ordination by partial detrended canonical correspondence analysis, principal components analysis and redundancy analysis (version 2.1). Technical Report LWA-88-02. Agricultural Mathematics Group, Wageningen.
- Turetsky, M., Manning, S., Wieder, R.K. (2004) Dating recent peat deposits. *Wetlands* 24(2), 324-356.
- Van de Vijver, B., Beyens, L. (1997) The epiphytic diatom flora of mosses from Stromness Bay area, South Georgia. *Polar Biology* 17(6), 492-501.
- Waddington, J.M., Morris, P.J., Kettridge, N., Granath, G., Thompson, D.K., Moore, P.A. (2015) Hydrological feedbacks in northern peatlands. *Ecohydrology* 8(1), 113-127.

- Wang, F., Xu, S. (2007) Characteristics analysis and trend forecast of drought and flood in Northeast China. *Journal of Dalian University of Technology* 47(05), 735-739.
- Zhang, H., Amesbury Matthew, J., Ronkainen, T., Charman Dan, J., Gallego-Sala Angela, V., VÄliranta, M. (2017) Testate amoeba as palaeohydrological indicators in the permafrost peatlands of north-east European Russia and Finnish Lapland. *Journal of Quaternary Science* 32(7), 976-988.
- Zhao, K. (1999) *Mires in China*, Science Press, Beijing.
- Zhang, M., Bu, Z., Jiang, M., Wang, S., Liu, S., Chen, X., Hao, J., Liao, W. (2019) The development of Hani peatland in the Changbai mountains (NE China) and its response to the variations of the East Asian summer monsoon. *Science of the Total Environment* 692, 818-832.

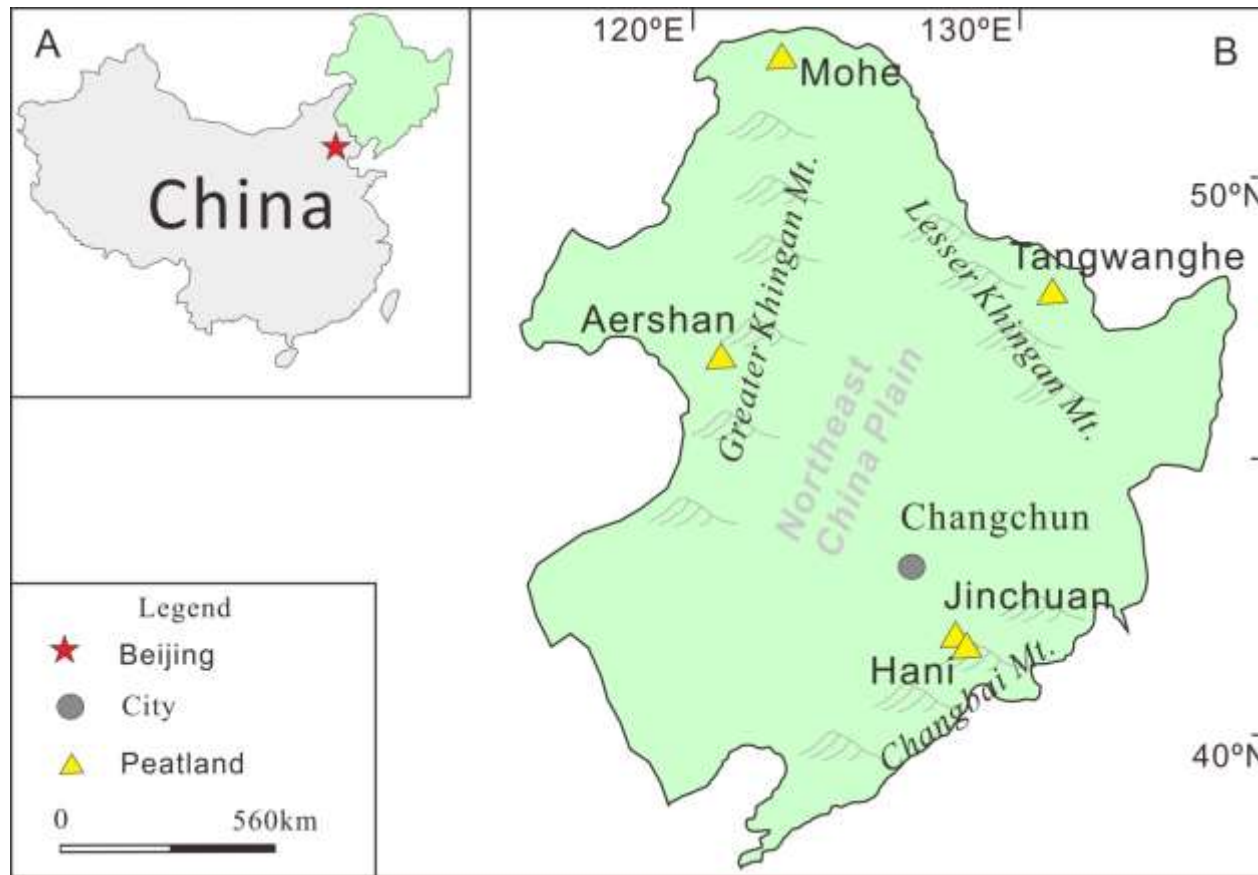


Figure 1 Locations of study area and sampling sites in China. Details for each peatland are listed in Table 1.

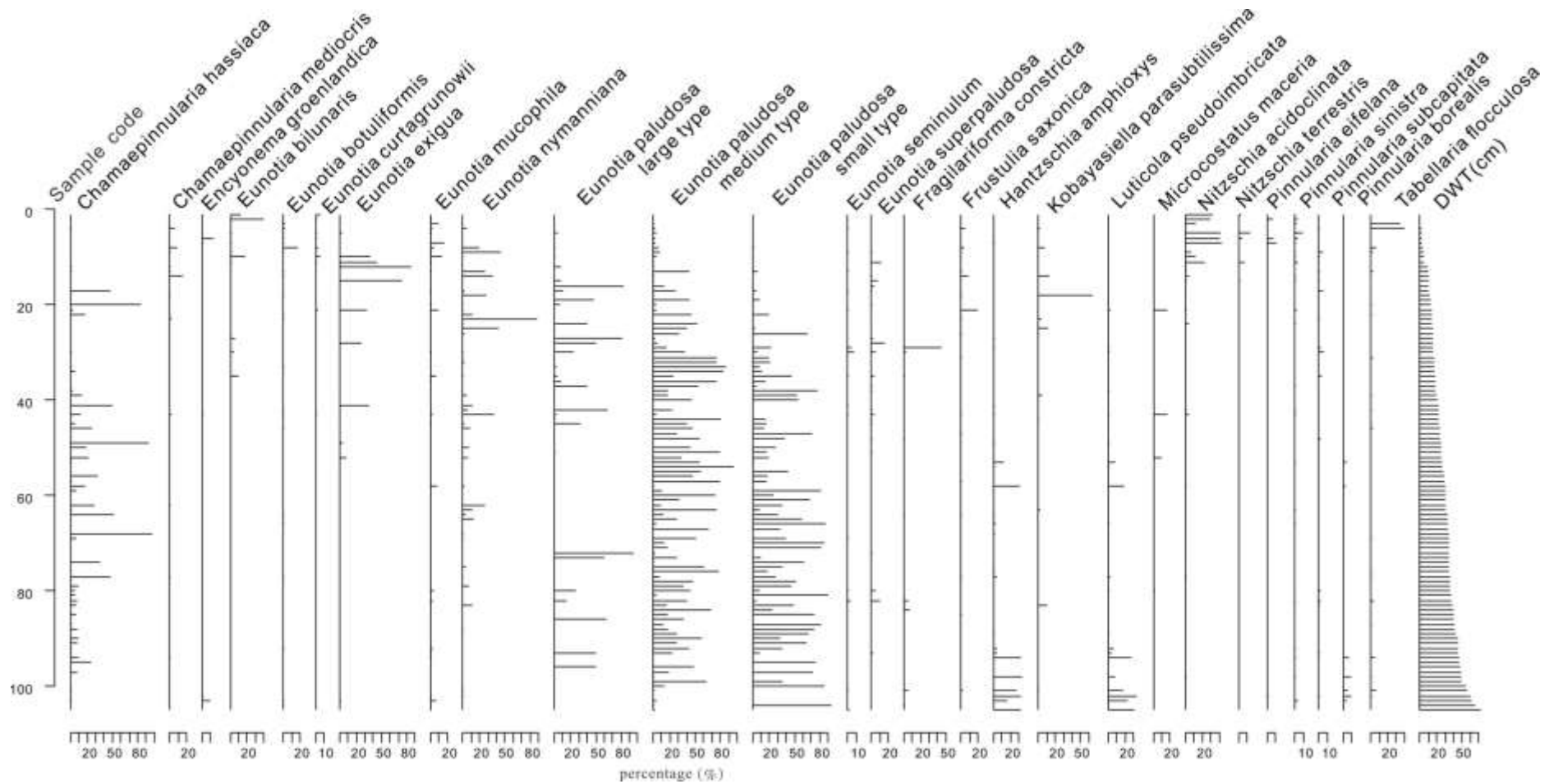


Figure 2 Relative percentage of main diatom taxa in modern samples plotted against depth to the water table (DWT).



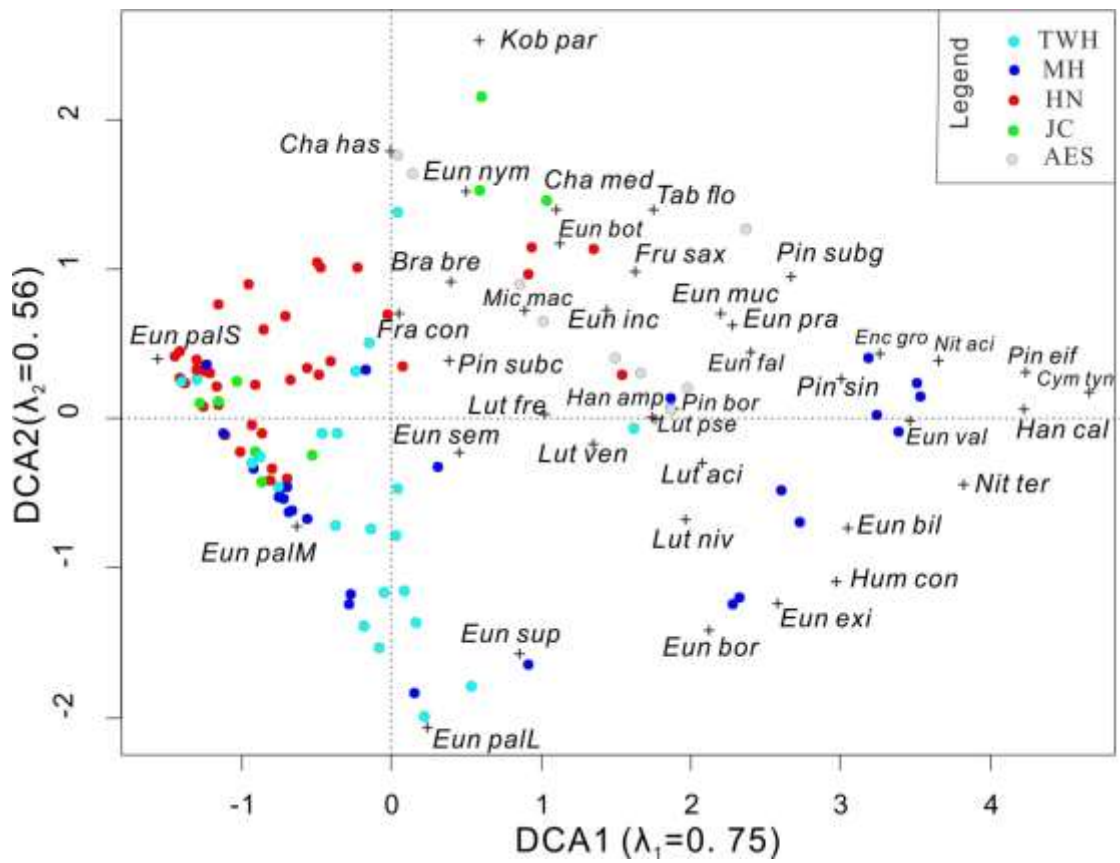


Figure 3 Detrended correspondence analysis (DCA) using 105 samples and 78 species, with main taxa shown. Species codes correspond to Appendix B.

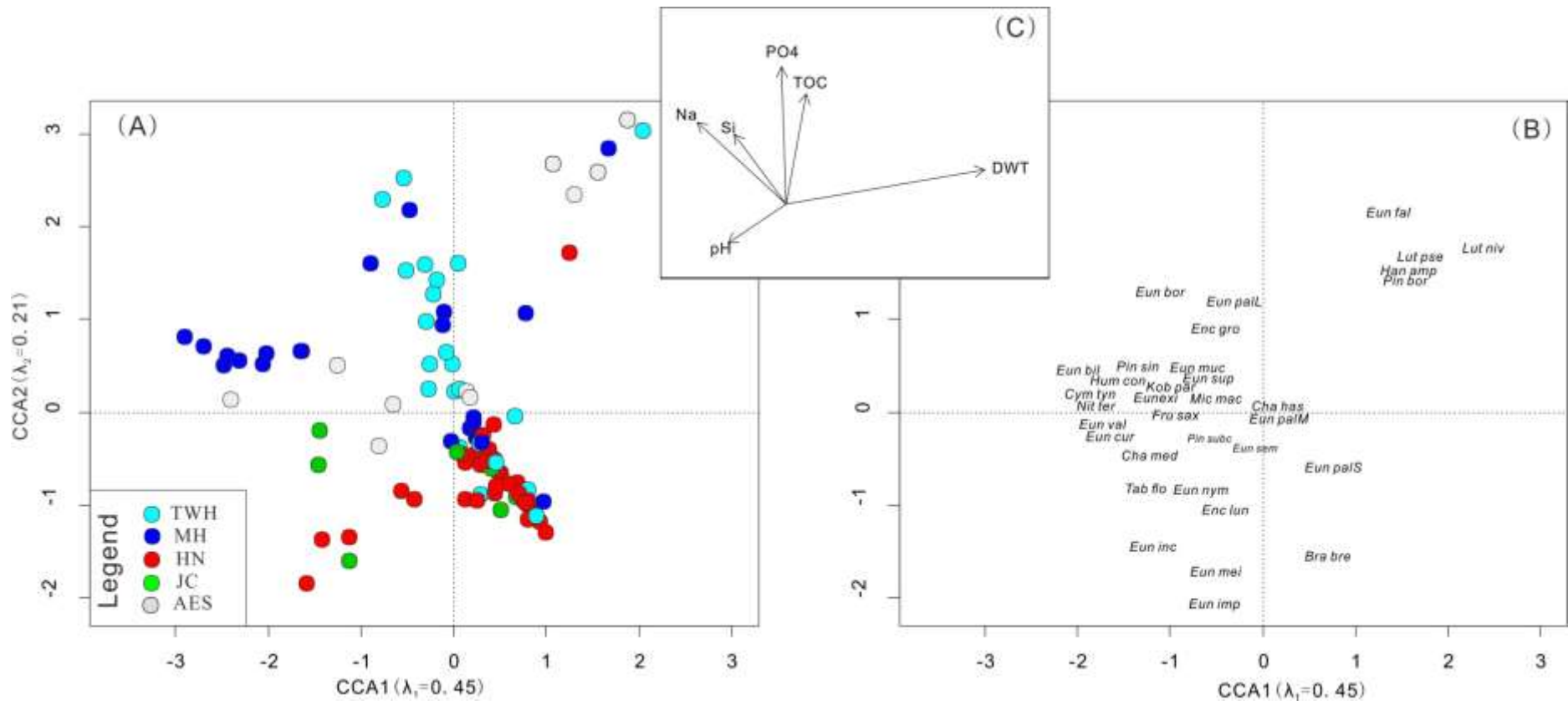


Figure 4 The biplots of canonical correspondence analysis (CCA) based on all 105 samples: samples (A), diatom species (B) and significant environmental variables (C). Taxon codes correspond to Appendix B.

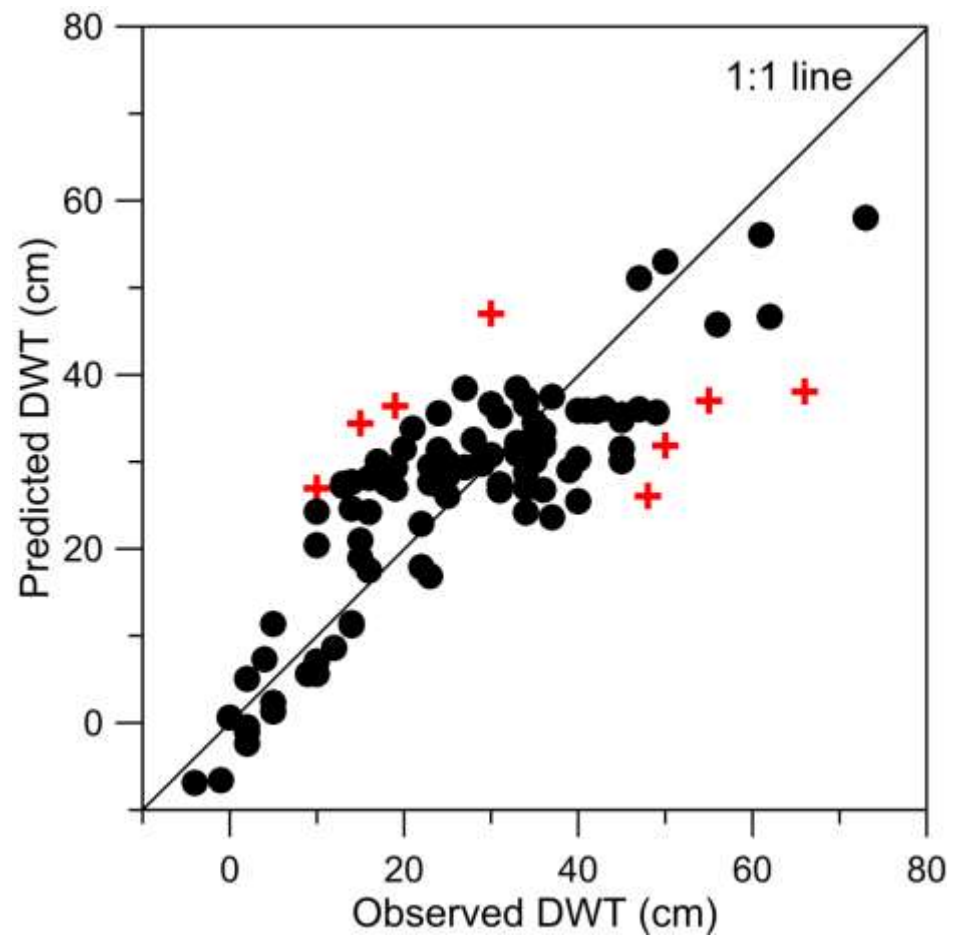


Figure 5 Observed versus WA.inv model-estimated depth to the water table (DWT) for the complete dataset. Red crosses represent samples with >20% residuals.

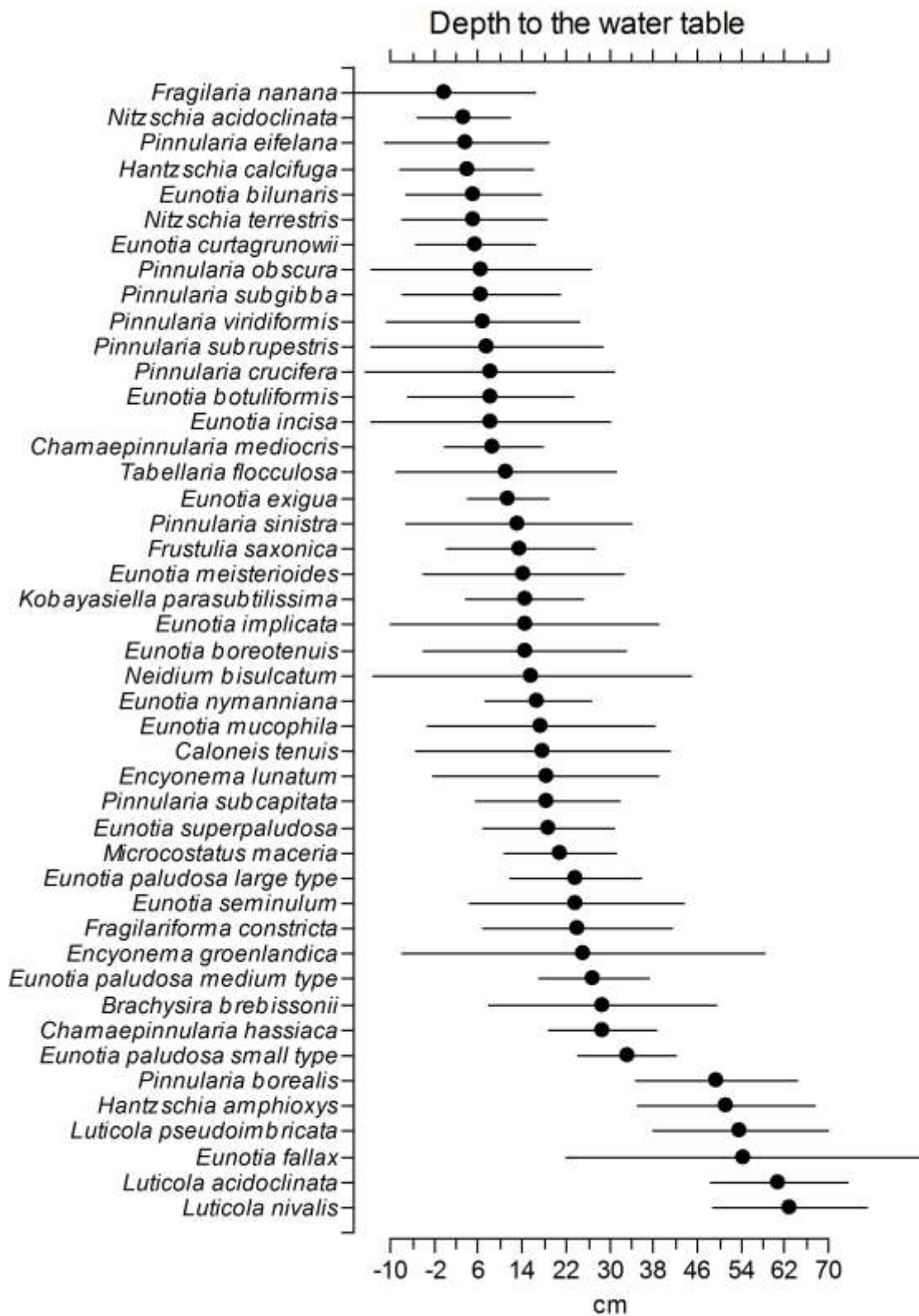


Figure 6 Optima and tolerance ranges for key diatom species along the water table gradient based on WA.inv model after removing samples with > 20% residuals.

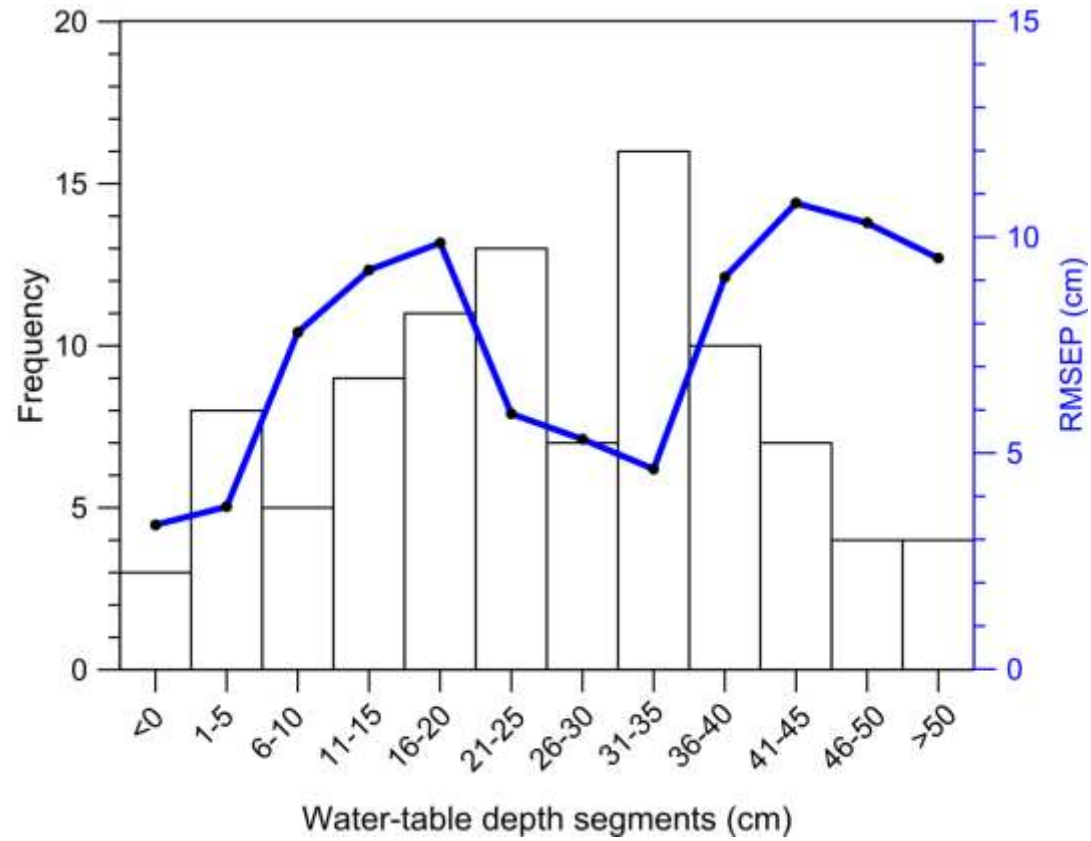


Figure 7 Sampling distribution of the dataset divided into 12 segments. Blue line shows segment-wise (SW) RMSEP for WA.inv model (calculation based on data removing residuals with >20% of overall DWT range).

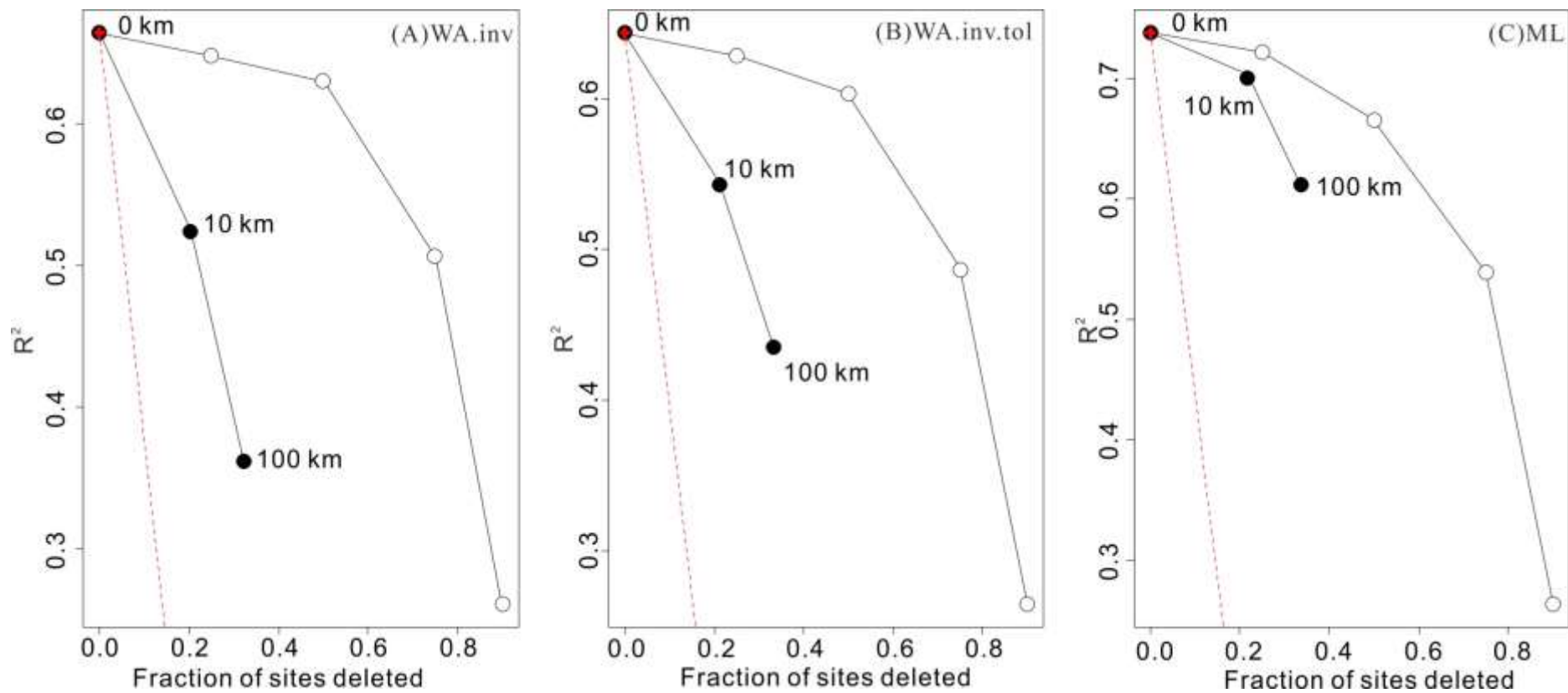


Figure 8 Plots showing the effect of spatial autocorrelation on transfer function  $R^2$  of deleting sites at random (open circles), from the geographical neighbourhood of the test site (filled circles) or that are most environmentally similar (red crosses) during cross-validation for WA.inv (A), WA.inv.tol (B) and ML (C).

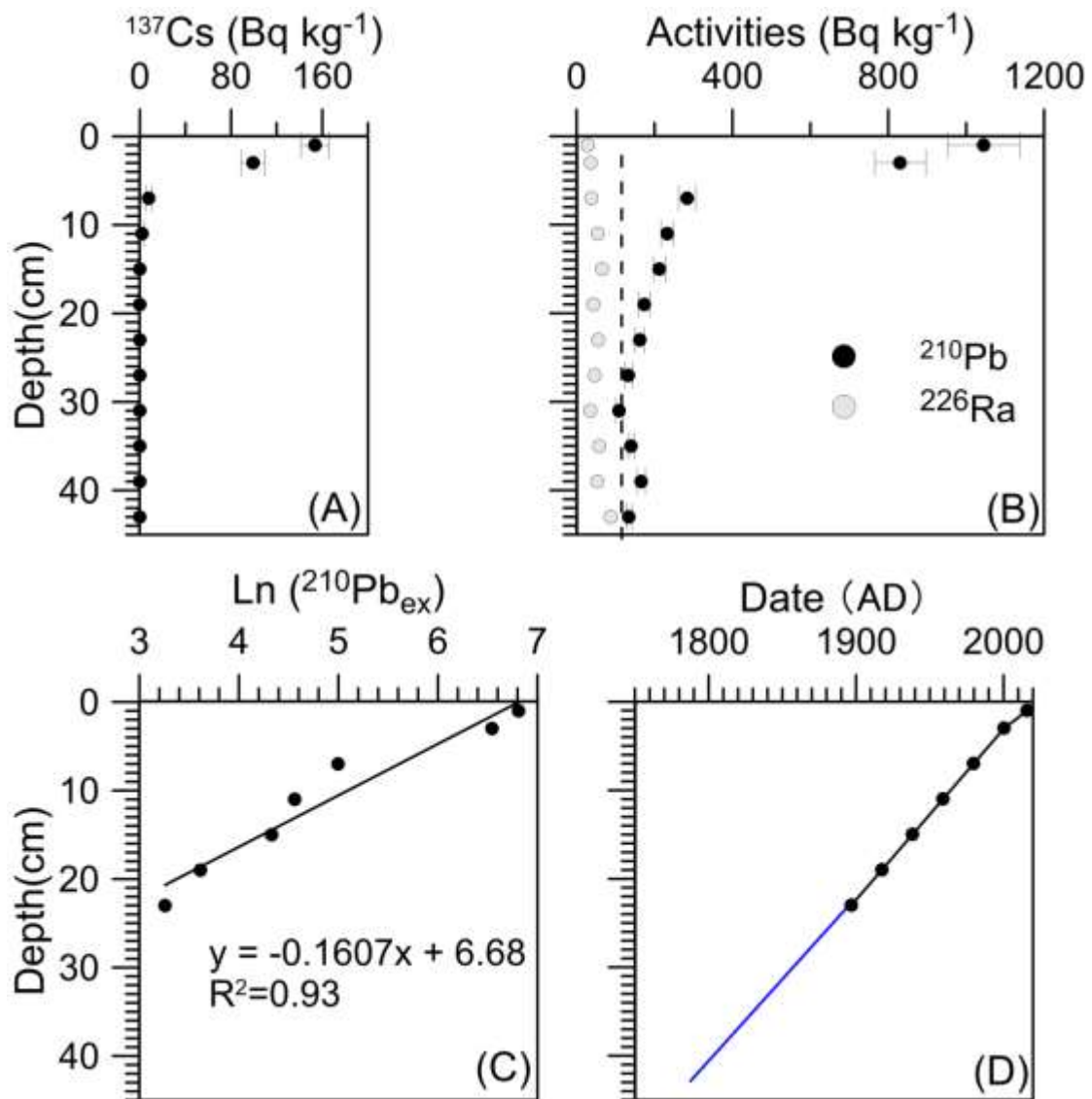


Figure 9 The activities of  $^{137}\text{Cs}$  (A),  $^{210}\text{Pb}_{\text{total}}$  and  $^{226}\text{Ra}$  (B), excess  $^{210}\text{Pb}$  ( $^{210}\text{Pb}_{\text{ex}}$ ) (C) and the dating results (D) in the Aershan peat core. The dashed line indicates a radioactive equilibrium of  $^{210}\text{Pb}_{\text{total}}$  activity. The blue line represents the age-depth relationship beyond the limit of  $^{210}\text{Pb}$  dating.

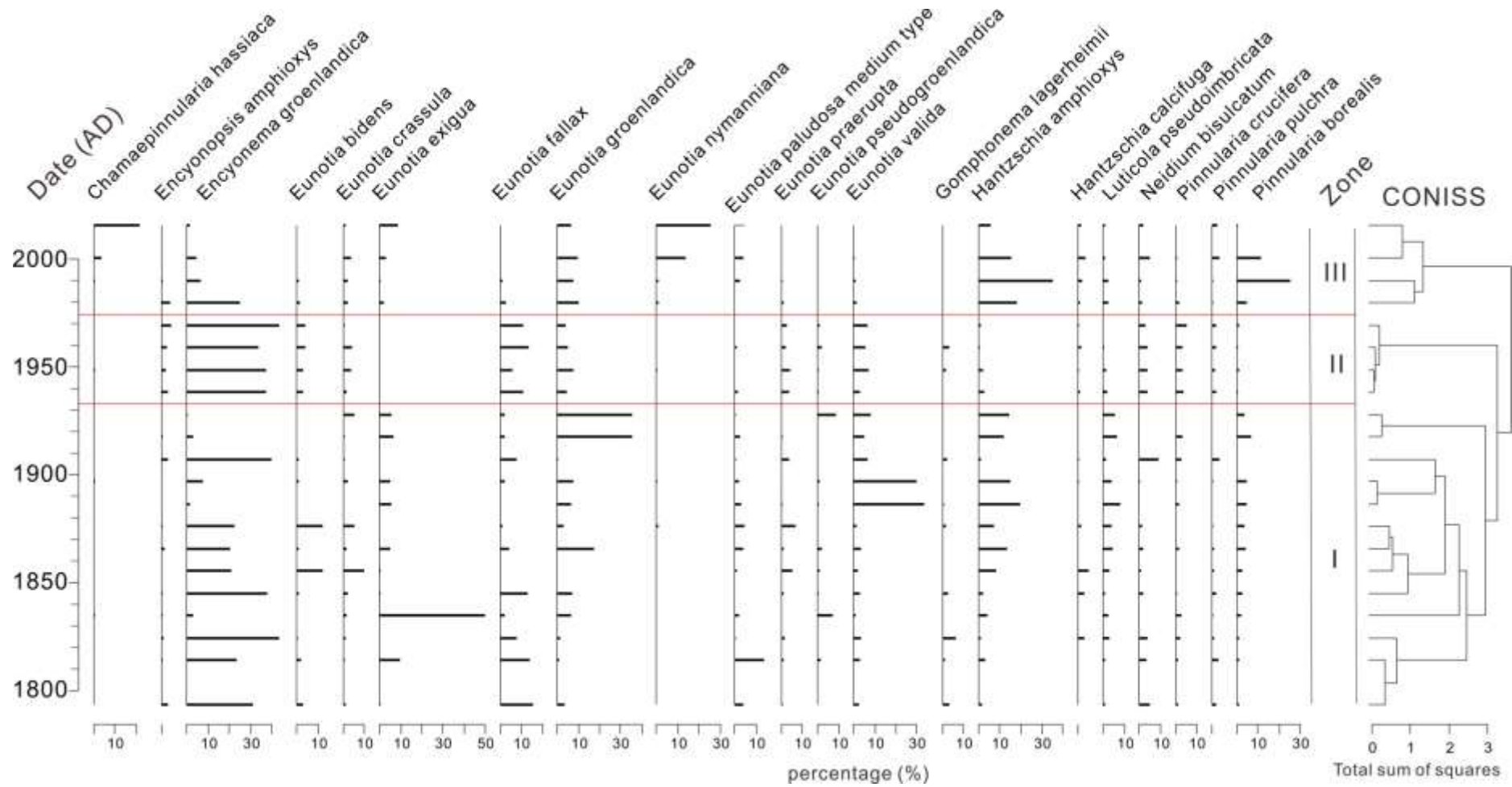
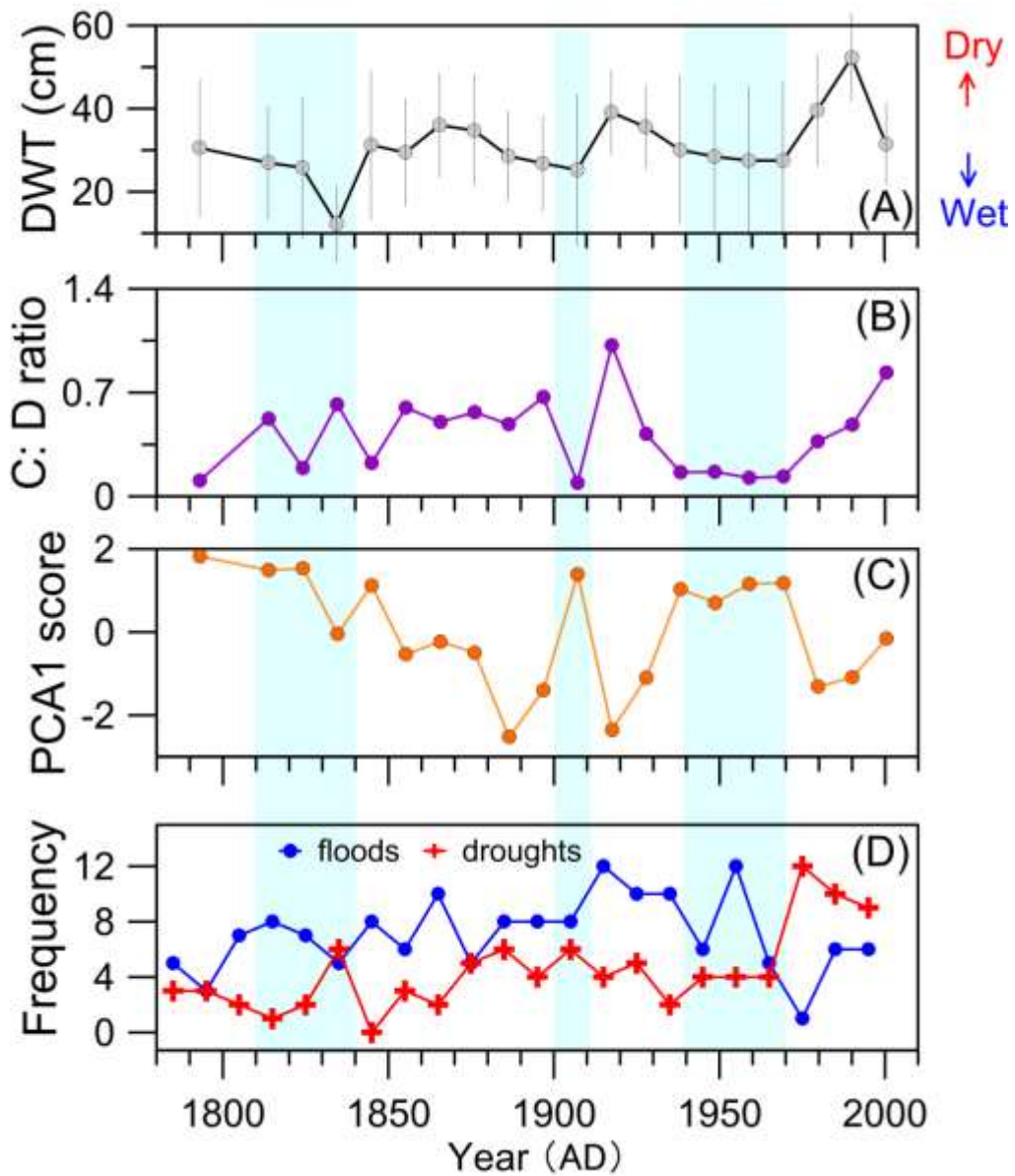


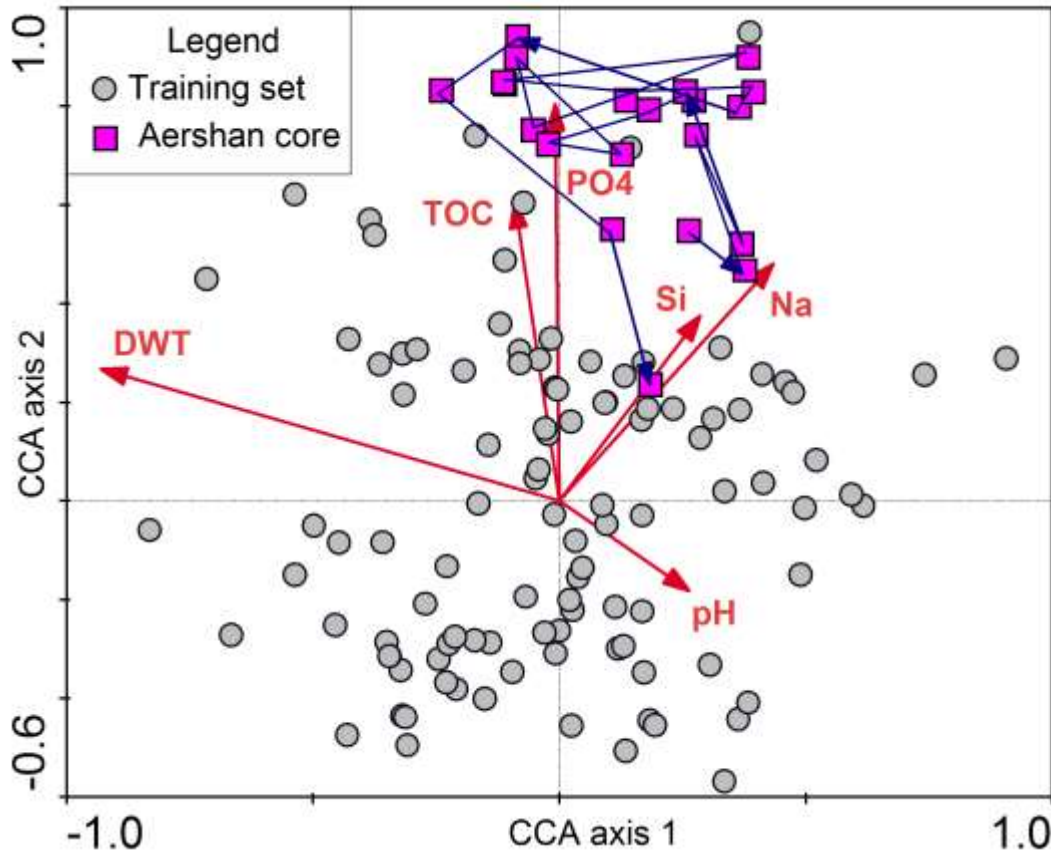
Figure 10 Diatom assemblages in the Aershan peat core with major taxa shown.





1

2 Figure 11 Sedimentary records in the Aershan peat core and regional climatic data,  
 3 including diatom-inferred DWT and standard error of prediction (A), the ratio of  
 4 chrysophyte cysts to diatom valves (B), sample scores on PCA axis 1 (C), and the  
 5 frequency of drought and flood events in northeastern China (D) sourced from Wang  
 6 and Xu (2007). The blue bars indicate wet episodes.



7

8 Figure 12 Biplot of the passive CCA with fossil samples passively plotted on the  
 9 modern training set.

10

11 Table 1 Details of sampling sites with the ranges of environmental parameters shown.

12 Mean annual temperature (MAT) and mean annual precipitation (MAP) data are from

13 Zhao (1999).

Site	Aershan	Mohe	Tangwanghe	Hani	Jinchuan
Code	AES	MH	TWH	HN	JC
Latitude (°N)	47°24'08.62"	53°08'12.05"	48°25'17.77"	42°13'31.52"	42°20'45.82"
Longitude (°E)	120°39'48.41"	122°02'50.11"	129°05'03.72"	126°31'13.15"	126°21'34.60"
Altitude (m a.s.l.)	1290	520	460	900	623
Area (ha)	30	-	-	1700	100
MAT (°C)	-3.1	-4.4	0	3.1	3.3
MAP (mm)	460	425	600	740	710
No. of samples	10	26	23	37	9
DWT (cm)	0-62	-4 to 50	10-73	2-66	10-35
pH	4.54-5.94	5.82-6.84	4.36-5.87	5.27-6.02	5.31-5.6
Cond ( $\mu\text{S cm}^{-1}$ )	26-78	19-74	26-70	22-61	38-60
ORP (mV)	196.4-332.5	194.7-321	209.1-329.2	141.5-312.5	223-236.5
$\text{PO}_4^{3-}$ ( $\mu\text{g L}^{-1}$ )	1-28	0-5	0-33	0-4	0-3
$\text{NO}_3^-$ ( $\mu\text{g L}^{-1}$ )	44-246	0-29	9-395	19-351	80-278
TOC ( $\text{mg L}^{-1}$ )	65.7-228.4	13.4-46.6	63.8-197.2	25.7-49.5	34.2-111.5
$\text{Ca}^{2+}$ ( $\text{mg L}^{-1}$ )	0.70-4.25	1.25-8.37	1.86-8.18	1.80-5.72	3.87-6.25
$\text{Na}^+$ ( $\text{mg L}^{-1}$ )	0.65-8.71	0.51-4.09	0.70-2.91	0.52-1.79	1.19-2.13
$\text{K}^+$ ( $\text{mg L}^{-1}$ )	0-5.6	0-0	0-12.3	0-1.60	0-0.42
$\text{Mg}^{2+}$ ( $\text{mg L}^{-1}$ )	0.30-2.45	0.23-2.71	0.45-2.68	0.50-2.04	1.28-2.09
Si ( $\text{mg L}^{-1}$ )	0.44-3.06	1.01-12.51	0.67-6.67	0.72-3.81	2.08-6.60

14

15

16 Table 2 Summary of the CCAs for marginal effects and unique effects of each  
 17 significant environmental variable.

Explanatory variable	Marginal effect			Unique effect	
	Eigenvalue ( $\lambda_1$ )	Eigenvalue ( $\lambda_2$ )	$\lambda_1/\lambda_2$ ratio	Variance explained	p-value
DWT	0.3139	0.565	0.56	4.99	0.001
Na <sup>+</sup>	0.1737	0.526	0.33	1.72	0.021
Si	0.1141	0.5787	0.197	2.16	0.002
TOC	0.1181	0.5895	0.2	1.7	0.012
pH	0.1246	0.5778	0.22	1.97	0.004
PO <sub>4</sub> <sup>3-</sup>	0.1267	0.5768	0.22	1.35	0.058

18

19

20 Table 3 The performance statistics for the transfer functions with leave-one-out cross  
 21 validation. For each improved model, number of removed samples for each model is  
 22 shown in parentheses.

	RMSEP	$R^2$	Maximum bias(cm)
Model performance for all samples			
WA.inv	10.4	0.57	25.5
	<u>12.8</u>	<u>0.34</u>	<u>28.2</u>
WA.inv.tol	12.0	0.42	37.9
	<u>14.6</u>	<u>0.18</u>	<u>43.3</u>
ML	12.2	0.55	15.3
	<u>14.6</u>	<u>0.33</u>	<u>21.2</u>
Models re-run after removing residuals >20%			
DWT gradient			
WA.inv (8)	8.8	0.66	17.5
	<u>11.7</u>	<u>0.40</u>	<u>18.3</u>
WA.inv.tol (13)	9.6	0.52	32.5
	<u>10.1</u>	<u>0.48</u>	<u>16.9</u>
ML (18)	11.5	0.52	29.5
	<u>14.1</u>	<u>0.34</u>	<u>69.4</u>

23 Normal: leave-one-out cross validation. Underline: leave-one-site-out cross  
 24 validation.

25

26